

SOLAR FLARE CYCLES

G. MARIŞ¹, M. D. POPESCU^{1,2}

¹*Astronomical Institute of the Romanian Academy
Str. Cutitul de Argint nr. 5, RO-752121, Bucharest, Romania
gmaris@aira.astro.ro*

²*Armagh Observatory
College Hill, Armagh, BT61 9DG, N. Ireland
mdp@star.arm.ac.uk*

Abstract. We present a review of different solar flare periodicity intervals. Our analysis includes a statistical investigation of flare occurrence and N-S hemispheric distribution over the last three 11-yr solar cycles (SCs 21-23, corresponding to the period 1976-2001). Moreover, we try to estimate if there is any connection between the flare activity and the strength of solar cycles. For that purpose, we studied not only the number of flares occurring monthly and annually, but we also used two indices that estimate the energy emitted by flares registered in the optical H_α line, as well as in the soft X-ray 1-8 Å band. The strange behaviour of SC 22 descending phase, with short but intense increments in flare activity, having a high degree of N-S asymmetry, could be the cause of the "abnormal" appearance of SC 23. The new magnetic dipole begins to lose part of its energy even during the descending phase of SC 22, so that the activity of SC 23 proves to be below the predicted values.

Key words: Sun – solar flares – solar activity cycles – N-S asymmetry.

1. INTRODUCTION

Solar flares are wonderfully complex phenomena, seen as sudden and intense increases in brightness on the solar disk. They occur when magnetic field loops undergo reorganization, releasing energy into the solar coronal and chromospheric plasma. It is widely accepted that they are the result of the rapid conversion of a large amount of magnetic energy, previously stored in the solar corona, and dissipated through magnetic reconnections. The release of energy takes place in a matter of minutes to a hours, and can amount to values up to 10^{26} J (10^{33} erg). The resulted electromagnetic radiation can extend over a very broad range of wavelengths, from gamma rays at the shortest wavelengths to radio waves at the long-wavelength end of the spectrum. The energy released heats the surrounding

plasma to temperatures that could be as high as 50×10^9 K, representing the highest temperatures that plasma can reach in the solar atmosphere. It is now well known that flares act as very efficient particle accelerators. Through the electric fields associated with the varying magnetic fields that are characteristic for such magnetically complex active regions, electrons and ions could be accelerated to energies up to 100 MeV.

The first flare was detected independently by R. C. Carrington as well as R. Hodgson on 1 September 1859. It was seen as a local and short-duration brightening on the white light image of the Sun. Nevertheless, flare data were very scarce for more than seven decades, as not many flares release as much energy so that to be seen in the continuum.

Following G. E. Hale's invention of the spectrohelioscope during the 1920s, flares began to be studied in the optical H_α emission line, being continuously monitored at this wavelength from ground stations since 1936. With the advent of space-based observations, flares have been observed throughout the short end of the electromagnetic spectrum, from ultraviolet through to gamma rays. Since 1975 they are continuously registered also in soft X-ray (SXR; 1-8 Å), complementary to the "classic" H_α line patrolling.

Not surprisingly, the successive opening of new observational windows to the flare phenomenon has resulted in the development of classification schemes particular to given wavelengths. These classification schemes encompass flare size and morphology, and, in the case of flare-associated energetic particles, the particle composition.

There are two widely used classification systems that address flare "size" or "importance". The first of these is the H_α classification scheme that was developed during the 1930s. It consists of a character (S = subflare, or 1, 2, 3 and 4 for successively larger flares) that denotes the flare size, and a letter (f = faint, n = normal, b = bright) corresponding to a subjective estimate of the emission intensity. Thus, the most outstanding flares are classified as 4b and the smallest and faintest as Sf.

A second classification that has come into common usage since about 1970 is based on SXR observations of the Sun in the 1-8 Å band by Earth-orbiting satellites. The size of the flare is given by the peak intensity (on a logarithmic scale) of the emission. Flares are classified with a letter (A, B, C, M or X) corresponding to the power of 10 (-8, -7, -6, -5, -4, respectively) of the peak 1-8 Å flux in units of Wm^{-2} and a number (1-9) that acts as a multiplier. When flares occasionally exceed class X9 in intensity, they are referred to as X10, X11 etc. events.

Continuous flare observations are very important not only for solar studies but also for the consequences they have in the heliosphere, which affect the Earth environment from the outer limits of the magnetosphere to the ground. In the near-Earth space environment, flares cause immediate increases in the flux of ionizing radiation such as highly energetic electrons, protons and photons. They are also correlated with delayed complex geomagnetic effects at Earth: the aurora and

temporary disruption of the Earth's magnetic field are generally observed 24–48 hours after the occurrence of a solar flare. This delay time corresponds to the transit time of the solar particles accelerated in the flare magnetic structures that propagate out from the Sun at about 1000 km/s (in comparison with only 300–400 km/s, the slow solar wind speed). However, flares are not the only solar phenomena associated with aurorae or geomagnetic storms (Mariş et al., 2002b [18]). Terrestrial magnetic disturbances are also caused by coronal mass ejections, sudden disappearing filaments, eruptive prominences or Earth-directed fast solar wind streams.

The interest in studying those fluctuations increased with the increasing usage of spatial and terrestrial technological systems, which are affected by such events. They can destroy satellites in low orbits, disrupt radio communications, cause damaging surges in long length power grids and corrode pipelines. For a more detailed description of space weather phenomena and associated terrestrial effects, see Popescu and Mariş, 2002 [21].

In this paper we investigate the flare occurrence as registered both in H_α and soft X-ray (SXR) during the period 1976–2001, representing the solar cycles (SCs) 21–23. For this purpose we use two types of flare indices: a frequency index (the total flare number, also divided on flare subclasses), as well as two importance indices that estimate the flare energy release for both types of flares considered. We use not only the H_α index, defined in 1952 by Kleczek [9], but also the SXR flare index recently introduced by Mariş et al. 2002b, 2002c [18, 19].

We begin in Section 2 with a description of flare periodicity, followed, in Section 3, by a presentation of the data, indices and method of analysis used. Our results structured as regards the 11-yr and 22-yr cycles, together with a study of the flare occurrence in the northern and southern solar hemispheres (the N-S asymmetry) are summarized in Section 4. The derived conclusions are given in Section 5.

2. FLARE PERIODICITY

Observations indicate that flare occurrence follows certain periodicity intervals. At a short-term scale, they undergo a 28-day periodicity, obviously related to the active region distribution on the solar disk. On longer-term intervals, several other cycles have been noticed to exist in the flare occurrence. They are reviewed in the following subsections.

2.1. Solar rotation period

The 28-day periodicity can very clearly be observed in "butterfly diagrams" that represent a graphical illustration of the flare positions in respect to the solar latitude and the time of their occurrence. One can see such a diagram, made for the

last two solar cycles, in Fig. 5 of Mariş et al., 2002c [19] (the "butterfly diagram" for X-ray flares, 1986–2001). A "nervure" structure appearing in both hemispheres from the highest to the lowest latitudes, with a temporal dimension of approximately 13–14 days, can be defined as a "fingerprint" of the flare occurrence. This structure is more evident if we made separately the diagram for different X-ray flare spectral classes (Fig. 1).

Fig. 1.

The butterfly diagram of H_{α} flares, plotted in Fig. 2, is very similar to the one of SXR flares. The representation of the butterfly diagrams on shorter intervals (e.g. only a few solar rotations) confirms the temporal dimension of this "nervure": approximately 13–14 days. This obvious agglomeration of flares for half a solar rotation period seems to be caused by the presence on the visible disk, at different latitudes, of some very flare-prolific active zones.

Fig. 2.

It was actually shown that more than 50% of flares occur in less than 4% solar area, namely in the "energetic flare zones", as defined by Verma et al., 1987 [25] or "superactive regions", as named by Bai, 1987, 1988 [4, 5]. Those are large, magnetically complex areas and thus very productive in energetic solar phenomena.

2.2. The 11-yr cycle

The 11-yr cycle, generally defined through the sunspot relative number, is the most evident periodicity that can be seen in all the solar atmospheric phenomena. It certainly represents the clearest periodicity observed also in flare behaviour, flares following the cycle evolution with their power and frequency of occurrence increasing towards the activity maximum. However, their time distribution is not the same as for sunspots. Generally, the flare cycle has a longer maximum phase; flares of small importance usually have their maximum before or coincident to the sunspots one, while the majority of more energetic flares occur later (Dinulescu and Dinulescu, 1991 [6]). On the descendant phase there are also some periods with increased flare activity, greater than for sunspots, especially for periods closer to the minimum. They represent the energy released mainly by small importance flares (Popescu et al., 2002 [22]), that probably appear because of the interaction between the magnetic fields on large as well as small scales, belonging to the old and respectively to the new solar cycle, with a reversed dipole. Most of those pulses from the descendent solar activity phases have geophysical effects on the terrestrial environment (Mariş et al., 2002b [18]).

2.3. The 22-yr magnetic (Hale) cycle

A 22-yr unit of solar periodicity has been taken into consideration since 1919, when G. E. Hale noted that the magnetic polarity of the preceding and the following spots of the bipolar regions reverse from one 11-yr cycle to the next, in each solar hemisphere. Moreover, the Sun's magnetic polarity reverses from a pole to the other after the sunspot maximum (Babcock and Babcock, 1955 [3]). This magnetic cycle, composed of two (statistically defined) 11-yr cycles, represents, in fact, the Sun's "physically true" cycle (Mariş et al., 2001 [16]). It is also referred to as the Hale cycle (HC).

The majority of HCs seemed to follow a certain "rule": the second 11-yr cycle of the pair is expected to be more powerful. This is known as the Gnevyshev-Ohl rule (G-O rule; Gnevyshev and Ohl, 1948 [8]) but, for the first time in the last 140 years, it is now being broken.

Because of this empirical rule, it was generally predicted, for the current 11-yr cycle, a much higher value for the smoothed sunspot number, as well as for other solar activity indices. Moreover, based on the G-O rule predictions, it was expected that the SC 23 would be the highest ever observed. Surprisingly, the amplitude of the relative sunspot number was smaller for the current cycle than for the previous one (Mariş et al., 2000 [15]).

Generally, the relative sunspot number most commonly defines the aspect and strength of a solar cycle, because it is the index with the longest record in history. Other indices of solar activity display, in general, similar trends, but not always. For example, the total solar irradiance displays a similar value for the current maximum as for the previous one (as noted by Jones et al., 2003 [12]). If this observation is not affected by any uncompensated systematic instrumental effects, it is quite a surprise that the Sun did not undergo any increase in its total energy output. Such an increase is expected to be detectable with the precision of the nowadays instruments, due to the fact that it is supposed to become hotter and hotter.

Flare occurrence apparently had a higher maximum in the current 11-yr SC than the previous one, contrary to the sunspots. Nevertheless, as we will show later in the paper, flares of small importance imposed this tendency. The total number of flares is indeed higher in the current cycle, but when looking at other flare indices that estimate the amount of energy released, their values are smaller comparing to the previous cycle. Flare behaviour in relation to the 22-yr cycle is therefore more complex.

2.4. North-South asymmetry

A longer-term periodicity was observed in the occurrence of flares, especially related to their distribution on the solar disk.

Activity features from the entire solar atmosphere do not occur uniformly on

the solar disk, more events appearing in one or other hemisphere during certain periods of time. Concerning flare hemispheric distribution throughout the cycles, the same behaviour as seen in all other solar activity phenomena can be inferred. Moreover, studies on the flare distribution seem to be very important, as magnetically active regions producing flares and regions with low activity could originate from different levels of the convection zone (Bai, 1987; 1988 [4, 5]). The asymmetry of solar flares could therefore add precious information to the solar dynamo theory.

A periodicity of about 11-12 years was found in flare hemispheric distribution, but whether or not it is related to the classical sunspot cycle is still controversial. Most of the authors that studied this subject concluded, nevertheless, that the asymmetry is not in phase with the 11-yr SC (e.g., Garcia, 1990 [7]; Vizoso and Ballester, 1990 [27]; Temmer et al., 2001 [23]). Longer-term periods were also suggested: 8 SCs (Vizoso and Ballester, 1990 [27]; Ataç and Özgüç, 1996 [1]) and even 12 SCs (Verma, 1992 [26]; Li et al., 2002 [13]).

However, based on such studies, the asymmetry of the solar activity in the present SC should favour the southern hemisphere, but current data suggest otherwise (see Sect. 4.2).

3. DATA AND METHODS

The number of different types of flares was often used as index in statistical studies of flare occurrence or flare N-S asymmetry. This index reflects how frequently solar flares appear during one interval or in one solar hemisphere and give little information about the associated energy release. Its main time variation is the 11-yr cycle.

Other types of indices, which contain more information on the importance of these phenomena, are also used to evaluate the energy released by flares (e.g. Knoska, 1985 [10]; Mariş, 1987 [14]; Ataç and Özgüç, 1996; 2001 [1, 2]). Such indices prove more useful in the analysis of flare spatial distribution, and reveal flare concentrations in active longitudes or in one solar hemisphere (N or S; N-S asymmetry). In fact, there are two different classes of indices: frequency indices and importance indices (Kuklin, 1976 [11]).

We are analysing here the energy released by both H_{α} and SXR flares during the last three solar cycles (the period 1976-2001), using two types of indices that evaluate it: the Q index for H_{α} flares and the Q_x index for SXR flares. We study the monthly, as well as the annual values of their distribution. Data used in this study were provided by WDC-A for Solar-Terrestrial Physics, NOAA E/GC2, Broadway, Boulder Colorado.

The Q index, computed by Ataç and Özgüç, 1996; 2001 [1, 2] from January 1976 to July 2000, was defined by Kleczek, (1952) [9] for describing the H_{α} flare activity over a 24 hour period, as:

$$Q = i \times t, \quad (1)$$

where i represents the intensity scale of importance of a flare in H_α and t the duration of the flare in minutes. It is assumed that this relationship evaluates roughly the total energy emitted by flares in the H_α line.

Flares also emit an important amount of energy in soft X-ray. For estimating the flare energy release in the 1–8 Å band, we quantified them over a period of 24 hours. Thus, we calculated the index Q_x defined by Mariş et al. (2002b; 2002c [18, 19]) through:

$$Q_x = i_x \cdot t, \quad (2)$$

where i_x is the intensity scale of importance of the X-ray flare spectral class. To obtain final daily values, the daily sums of the index for all SXR flares are divided by the sums of total flare duration for that day. We defined i_x as in Table 1, based on the classification of solar flares according to the magnitude order of the peak burst intensity within 1–8 Å, measured from Earth-orbit. This evaluation is similar to that carried out on H_α flares energy release.

There is a difference between the indices derived from the two different kinds of flare classification: the Q index is defined using the area covered by flares in H_α while the Q_x index is defined using the energy emitted at the maximum phase in 1–8 Å by SXR flares.

The Q_x index as a good indicator for the importance of SXR flares, e.g. an importance index. Moreover, we consider that it helps comparing the two classes of flares, by providing information on the energy released by the X-ray flares.

Table 1.
The i_x coefficient values for the different spectral classes of SXR flares.

SXR class	i_x
B	0.5
1.1-5.0 C	1.0
5.1-9.9 C	1.5
1.1-5.0 M	2.0
5.1-9.9 M	2.5
1.1-5.0 X	3.0
> 5.1 X	3.5

We first analyse the time distribution for SXR and H_α flares, by the monthly number of the events for the period January 1986 – March 2001. We overviewed their monthly distribution by splitting them into two categories. The histograms

representing the monthly number of flares for each category are plotted in Fig. 3, as follows:

- upper panel: medium energetic – C type (12,146 events);
- middle panel: high energetic – M and X type (2,809 events);
- lower panel: C, M and X type (14,955 events).

Because the energy emitted by the low energetic flares (B and A type) is very small (3, respectively 4 orders of magnitude smaller than for the X type) we did not introduce them in the total flare counting.

Such statistics help us evaluating the flare occurrence during the present HC (the period 1986–2001).

Fig. 3.

In Fig. 4 we present the monthly variation of the Q_x and Q indices during the present HC. This plot underlines the importance of the flares registered both in SXR (through the energy emitted at 1-8 Å) and H_α band (through the area of each event).

Fig. 4.

In order to have a larger span of data for our analysis, we extended the monthly and yearly values of the Q_x and Q indices with one more 11-yr cycle (SC 21). We now have a data set of 25 years (1976 – 2001).

Moreover, for better inferring the cycle characteristics of our indices, we calculated the smoothed monthly mean values for Q_x and Q . This smoothing method is also used for the sunspot relative number in forecasting studies, because it eliminates the seasonal variations. The monthly smoothed values are calculated according to:

$$Q_s = \frac{Q_{i-6} + Q_{i+6} + 2 \sum_{j=i-5}^{i+5} Q_j}{24} \quad (3)$$

The smoothed values of the two indices, (magnified by 10 for the Q index and by 100, for the Q_x index), are given in Fig. 5, where one can also see, for comparison, the smoothed sunspot numbers.

Fig. 5.

In addition to the monthly distributions, we have also considered the annual values of the flare indices for the extended period of time. The histograms are plotted in Fig. 6, which also displays the annual sunspot relative number. The difference in the level of flare activity and in the slope and the duration of each phase for the last three SCs is beautifully seen as regards the yearly trends of both

indices.

Fig. 6.

Generally, for a given index, C , separately determined for both solar hemispheres, one can calculate two almost equivalent asymmetry indices:

$$a = \frac{C_N}{C_S} \text{ and } A = \frac{C_N - C_S}{C_N + C_S} \quad (4)$$

We have chosen the A index for our studies of flare asymmetry during the last three SCs, and we have calculated it for the SXR flare number (N), as well as for the Q_x index.

We have therefore evaluated the degree of N-S asymmetrical distribution for the SXR flares (classes B, C, M and X) using the index of type A defined for the number of SXR flares, as:

$$A_N = \frac{N_N - N_S}{N_N + N_S}, \quad (5)$$

where N_N and N_S represent the number of flares in the northern and southern solar hemispheres, respectively. The A_N values were calculated both monthly and annually.

We have estimated the N-S asymmetry of SXR flares for the importance index Q_x , by the asymmetry index, A_Q , defined as:

$$A_Q = \frac{Q_N - Q_S}{Q_N + Q_S}, \quad (6)$$

The monthly degree of flare asymmetry, described by the A_N and A_Q indices, is further presented. In Fig. 7 we have plotted their smoothed values in order to mark out the trend of the asymmetry.

Fig. 7.

In Fig. 8 we evaluate the annual N-S asymmetry of the indices used, N and

Q_x , as calculated with formulas (5) and (6), respectively.

Fig. 8.

4. ANALYSYS OF THE RESULTS

4.1. The 11- and 22-year cycles

4.1.1. Flare numbers

The histograms representing the monthly number of C, M and X-type SXR flares during the last HC (the period January 1986 – March 2001) show the following characteristics the pair of the 11-yr cycles considered (see Fig. 3):

- For SC 22, SXR flares showed a remarkable increase during 1988, a high activity during the following two years (1988–1989) and a second maximum during 1991. After 1991, the activity began the descendent phase but had a sudden growth for the period June 1994 – May 1995. The whole cycle is characterized by an alternation of the activity between C-type and M & X-type solar flares.
- For the SC 23, the activity increased after the end of 1997 for both classes of SXR flares, until the year of maximum (2000). The high flare activity after November 1999 could be remarked. The most intense C-type flare occurrence took place in March 2000 (with a number of 303 flares of this type). Four maxima are revealed for the M & X-class of flares in November 1999 (41 M & X-class flares), March 2000 (40 flares), July 2000 (54 flares) and March 2001 (38 flares), the third being the most prominent.

We have found a very similar behaviour also for the H_α flares. A more detailed statistical analysis for this type of flares is given by Temmer et al., 2001 [23].

4.1.2. Flare importance indices. I. Monthly values

In Fig. 4 one can see the aspect of the importance indices during the present magnetic cycle. There is a large maximum period of flare occurrence for both the 22nd and the 23rd SCs. As more largely discussed in Popescu et al., 2002 [22], Q_x periods of maximum are even wider than for the Q index.

For SC 22, the double maximum structure of Q_x is present as it was for the Q index. Other characteristics are the pulses of higher activity on the descendent phase and the oscillations during the minimum.

When looking at the general layout of the importance indices (Fig. 4), one

can notice that their values are smaller for the current 11-yr cycle in comparison to the previous one. That behaviour is in contradiction to the one displayed by the total number of SXR flares, which has a higher maximum in SC 23 than in SC 22. Nevertheless, as it can very easily be inferred from Fig. 3 (upper panel), this trend was imposed by C-class flares, who release a small amount of energy. Actually, the contribution of C-class SXR flares to the Q_x index is of about 43%, and hence M and X flares influence more the index appearance.

4.1.3. Flare importance indices. II. Mediated values

In order to evaluate the flare activity during the last three solar cycles, we calculated the mediated values of Q and Q_x indices. The analysis was done for the total length (T) as well as for the ascending (A) and descending (D) phases of each cycle. These mediated values (Q_m and $Q_{x,m}$) were obtained by summing the values of Q and Q_x indices for each period considered, and then dividing it by the number of the months of the selected interval.

As one can see in Table 2, Q_m values are bigger for SC 21 than for SC 22 while the $Q_{x,m}$ values are exactly the same for both cycles. For SC 23 we do not have enough data for all estimations, and therefore we calculated Q_m and $Q_{x,m}$ for only for the ascending phase. The $Q_{x,m}$ value for the ascending phase of SC 23 is comparable with the corresponding values of SCs 21 and 22, while the Q_m value for SC23 is much smaller than for SCs 21 and 22.

Table 2.
The mediated values of the Q and Q_x indices for the total length (T), the ascending (A) and descending (D) phases of SCs 21 – 23.

SC	phase	period	Q_m	$Q_{x,m}$
21	T	Jun. 1976 – Aug. 1986	9.33	0.81
	A	Jun. 1976 – Nov. 1979	8.13	0.73
	D	Dec. 1979 – Aug. 1986	9.95	0.85
22	T	Sep. 1986 – Sept. 1996	6.99	0.81
	A	Sept. 1986 – Jun. 1989	7.17	0.81
	D	Jul. 1989 – Sept. 1996	6.92	0.81
23	A	Oct. 1996 – Mar. 2000	3.69	0.73

We also evaluated the maximum phases (M) of SCs 21 and 22 by the mediated values, calculated for four years and 10 months for the first cycle and four years, respectively, for the second one (see Table 3). The obtained values of Q_m and $Q_{x,m}$ are practically equal for the two cycles but higher than their values for other phases or for the whole length of cycles.

As previously noted, the descendant phases of both SCs 21 and 22 present some sudden growths (“pulses”) of flare activity. The indices mediated values during these periods are also given in Table 3. One can observe that the values for both pulses of SC 21 are comparable to the index mediated value over the whole

cycle. The same observation is valid also for the first pulse of SC 22, but the following pulses are much lower.

Table 3.
The mediated values of the Q and Q_x indices during the maximum phases (M1, M2) and the “pulses” on the descending phase for SCs 21(P1, P2) and 22 (P3-P5).

SC		period	Q_m	$Q_{x,m}$
21	M1	Feb. 1978 – Dec.1982	15.69	1.22
	P1	May – Oct. 1983	8.90	1.00
	P2	Jan. – May 1984	9.76	1.10
22	M2	Feb.1988– Feb.1992	14.74	1.40
	P3	Feb. – Jun. 1993	6.75	1.00
	P4	Oct. 1993 – Mar. 1994	2.92	0.65
	P5	Jun. – Oct. 1994	1.34	0.35

4.1.4. Flare importance indices. III. Smoothed values

From the smoothed values of $H\alpha$, respectively SXR flare indices (Fig. 5) it can be inferred the trend of the SCs, regarding the flare energy release, in comparison to the classical 11-yr cycle of sunspot number. For SC 21, it is clear that the maximum values of the indices for each flare type are delayed in respect to the sunspot numbers. For SC 22, the maxima happen simultaneously and show the same double-peak structure. For of SC 23, one can see that the maximum smoothed values for both the Q_x index and sunspot numbers are also temporally coincident and it seems that they will both have a second maximum.

4.1.5. Flare importance indices. IV. Annual values

In Fig. 6 we plotted the annual variation of $H\alpha$ and SXR flare indices for SCs 21–23 (gray and black histograms, respectively) together with the annual sunspot number.

The annual values of the $H\alpha$ flare index present, for SC 21, a maximum phase of four years during 1979–1982, with the highest value in 1982. SC 22 show a very sharp growth during the ascending phase and a double maximum profile for the years 1989 and 1991, the first peak being the highest. These epochs are coincident with the maximum ones for the sub-flares (in 1989) and the flares of importance ≥ 2 (in 1991), respectively. The minimum period between SC 22–23 is more prominent than for SCs 21–22. SC 23 presents a lower flare energy release on the ascending phase in comparison with SC 22 and also a steeper slope.

For the SXR flare index, the maximum phase of SC 21 is longer (five years, 1978–1982). SC 22 shows the same double maximum structure in 1989 and 1991, with the first peak higher, but closer to the value of the second one. The growth in the activity of SC 23 is stepper, due to the fact that during this cycle there are more flares of small importance. The annual value of the Q_x index for 2001 is slightly

higher than for the previous year, in contradiction to the annual sunspot number.

4.2. N-S asymmetry

We have analysed the N-S asymmetry of both flare types in order to check if there is any periodicity in their hemispheric occurrence. We made a comparison between the asymmetry of the total number of flares and the SXR flare index during the period 1976 – 2001 for their monthly distribution (Fig. 7), as well as for their smoothed values (Fig. 8).

In Fig. 8 we notice the near identical variation of the N-S asymmetry for the two indices, N and Q_x , even if they have a different nature (N is a frequency, and Q_x is an importance index).

A general trend can be inferred for the N-S asymmetry curve during a SC. At the beginning of a cycle, there is a preference for one of the hemispheres, while during, or immediately after the maximum epoch, the N-S asymmetry drops sharply towards zero and remains very low until the polarity reversal of the solar magnetic field. After this moment, in which a new dipole with inverse polarities is installed, the N-S asymmetry increases again, either in favour of the opposite hemisphere (for SC 21, it goes from North to South), or in favour of the same one (as for SC 22, where the southern hemisphere remains dominant). The current data of SC 23 does not allow us to yet infer which hemispheric preferences the flare activity will have on the descending phase of this cycle. Nevertheless, for the year 2001, the A_N and A_Q indices show that, even if in the southern hemisphere there were more SXR flares, the energy released by the northern ones was much greater.

The smoothed value curve allows the inference of a variation tendency. For a clearer picture of the asymmetry indices, we present in Fig. 7 the smoothed values of both the A_N and A_Q indices.

The two curves evolve nearly identically until July 1993. During the interval July 1993 – July 1997, they present an anti-phase evolution with short exceptions during the following periods: April–July 1994; April–July 1995; May–June 1996, which are strangely placed at one-year intervals. The inverse dynamics of the two indices is present again between October 2000 – July 2001. These periods correspond to the descendent phase of SC 22 and to the maximum phase of SC 23, respectively.

There is an explanation for the abnormal appearance of SC 23. During the years 2000–2001, a large number of very powerful SXR flares were registered, (e.g. the events of July 2000 and March–April 2001) as well as many small flares (C and B spectral classes). Mariş et al., 2002c [19] showed that during certain periods there is an alternation between the emergence of powerful SXR flares (X and M classes) and small importance flares (C class). When we calculated the daily Q_x index, we divided it by the total flare duration. Therefore, when there is a large

number of C and B class flares, the value of the Q_x index could be small, whereas when there are even few M and X class flares the index values increases.

In order to evaluate what can produce the anti-phase evolution of the two asymmetry indices on the descending phase of SC 22, we try to estimate the strength of an entire cycle, on different phases and during some evident "pulses" of activity, through a mediated value, $Q_{x,m}$. These values were obtained in the same manner as for the Tables 2 and 3, for three different intervals: the entire length (T) of the cycles, the ascending phase (A) and the descending phase (D). For SC 23, instead of the total duration of the cycle, we took into consideration only the period available, 1996–2001, and we left out the descending phase. Our calculation used the minimum and maximum epochs of the considered cycles given by WDC–A for Solar-Terrestrial Physics, NOAA. For the phases of SCs 21–23 we calculated the index $Q_{x,m}$, separately for the northern and southern hemispheres (Table 4). One can notice a southern dominance for SCs 21 and 22 with the exception of the ascending phase of SC 21. All the asymmetry values are relatively small irrespective of the cycle phase or the entire solar cycle.

Table 4.
The values of the $Q_{x,m}$ indices for the northern and southern hemispheres, during different phases of SCs 21–23.

SC	phase	period	hemisphere	$Q_{x,m}$	$A_Q_{x,m}$
21	T	Jun. 1976 – Aug. 1986	N	0.49	– 0.01
			S	0.50	
	A	Jun. 1976 – Nov. 1979	N	0.59	+ 0.19
			S	0.40	
	D	Dec. 1979 – Aug. 1986	N	0.51	– 0.11
			S	0.63	
22	T	Sep. 1986 – Sep. 1996	N	0.52	– 0.07
			S	0.60	
	A	Sep. 1986 – Jun. 1989	N	0.52	– 0.07
			S	0.60	
	D	Jul. 1989 – Sep. 1996	N	0.51	– 0.09
			S	0.61	
23		Oct. 1996 – Dec. 2001	N	0.56	+ 0.15
			S	0.41	
	A	Oct. 1996 – Mar. 2000	N	0.43	+ 0.01
			S	0.42	

SC 21 had a northern hemispheric dominance for the ascending phase, which shifted to the South for the second part of the cycle. For the entire cycle, we found a very weak southern dominance, as did most of other authors (see e.g. Temmer et al., 2002 [24]). For SC 22, our data show a southern preference, in agreement with other results from literature. One should notice the constant values of the $Q_{x,m}$

index in both hemispheres for both phases, and for the entire cycle. The main feature of SC 23 up to the year 2001 is a northern dominance of SXR flares, the same as for H α flares and the flare index.

We have also calculated $Q_{x,m}$ for the maximum phases of the cycles. We considered that the maximum phase begins in the month when the activity exceeded by 50% the level reached during the previous one and end in the month when the activity decreases by approximately 50% and then continues to go down.

Thus, we note the obtained periods with M in Table 5. The $Q_{x,m}$ value for the maximum phases of the solar cycles in both hemispheres shows the high energy level emitted by SXR flares in those periods, in comparison to the entire cycle or its ascending or descending phases alone. The N-S asymmetry during the maximum phase is almost zero, the value of the $Q_{x,m}$ index being practically the same as it is for the entire cycle (see row T in Table 4 and rows M in Table 5).

Table 5.

The values of the $Q_{x,m}$ indices for the northern and southern hemispheres, during the maximum phases and the "pulses" on the descending phase for SCs 21 and 22.

SC		Period	Hemisphere	$Q_{x,m}$	$A_{-}Q_{x,m}$
21	M	Sep 1978 – Dec 1982	N	0.91	+ 0.01
			S	0.89	
	Pulses	Mar–Oct 1983	N	0.28	– 0.50
			S	0.84	
		Jan–Jun 1984	N	0.53	– 0.12
			S	0.67	
22	M	Jun 1988 – Feb 1992	N	0.95	– 0.06
			S	1.08	
	Pulses	Feb 1993 – Jun 1993	N	0.67	+ 0.03
			S	0.63	
		Oct 1993 – Mar 1994	N	0.43	+ 0.28
			S	0.24	
		Jun–Oct 1994	N	0.13	– 0.27
			S	0.23	
23	M	May 1999 – Jan 2001	N	0.81	+ 0.05
			S	0.74	

The difficulty of analysing the "pulses" of activity on the descending phase starts from their definitions. In the panels of Fig. 4 these "pulses" can clearly be seen. Also, the data show that they do not appear simultaneously in the two hemispheres, but they present a certain delay. We have chosen to select the pulse intervals over the entire disk and to calculate the $Q_{x,m}$ index separately for both hemispheres, corresponding to these intervals (see Table 5).

The values obtained for the $Q_{x,m}$ index reveal an increased energy of the

SXR flare activity and a degree of asymmetry differing from that of the descending phase of the cycle. Therefore, even if in SC 21 the asymmetry is larger than in the descending phase, it keeps a southern dominance, while for SC 22 two of the pulses show a northern preference, contrary to the whole cycle, which is southern dominant. This could be due to a certain influence of the new magnetic dipole appearing after the polarity reversal. The northern dominance of the solar activity for SC 23, a feature also displayed by SXR flares, may confirm this hypothesis.

5. CONCLUSIONS

The study of flares is significant not only for better understanding the Sun, but also for learning about acceleration mechanisms of solar particles and being aware about the space weather phenomena they could trigger on the terrestrial environment. Forecasting space weather is extremely important, not only for the space missions having astronauts on board, but also for avoiding money losses due to damages that more and more spatial and terrestrial technological systems can suffer because of some space weather disturbances.

For over 35 years, the forecasts are continuously improved but there still are a lot of difficulties in making a complete, rapid and effective prediction of flare occurrence. Statistical studies of solar flare occurrence represent a valuable tool for improving their forecast methods both at short- and long-term time scales.

It is difficult to define an index that encompasses all the information about the flare phenomenon, especially evaluating the emitted energy. The number of flares reflects, unambiguously, the 11-yr solar activity cycle.

Attempting to evaluate through an index, as accurately as possible, the energy emitted by flares is useful for understanding the dynamical evolution of the solar magnetic field and of the solar cyclic activity, in general. Such an index exists since 1952 for H_α flares (Kleczeck, 1952 [9]). Even if flares begun to be registered also in SXR since 1975, from above the terrestrial atmosphere, a similar index that would reflect the importance of the events in this band was only recently introduced by Mariş et al. (2000b, 2000c [18, 19]). In this paper we extended its comparison with the total number of flares and with the H_α importance index.

In this context, our study leads to the following conclusions:

- Flares are better defined through importance indices, as regards the knowledge about the amount of energy released, then through frequency indices.
- H_α and SXR flare indices show a delay regarding the sunspot numbers for SC 21, while for SC 22 and 23 their time distribution is almost coincident.
- Even if from SC 21 to SC 23 there is a decrease in the energy emitted by H_α flares, as seen through the Q index, (see Q_m values in Table 2), the

amount of energy emitted by SXR flares, quantified through the Q_x index is about the same for all cycles (see $Q_{x,m}$ values in the same table).

- The degree of N-S asymmetry for both the frequency and the importance indices confirms the anti-phase SXR flare emergence for spectral classes M & X and, respectively, class C, noted by Mariş et al., 2000 [15].
- The degree of asymmetry for the Q_x index is constant during all phases of SC 22 and in the favour of the same hemisphere (South), while for SC 21 the asymmetry goes from North (ascendant phase) to South (descendant phase), even if with small values (see Table 4).
- The asymmetry of solar flares as regards the SXR importance index (see Table 5), is almost absent during the maximum phases of solar cycles, a feature identified by many authors, also for other flare indices.
- The evaluation of N-S asymmetry through mediated values of an importance index reveals only small differences between the two solar hemispheres (see Table 4). This may suggest the fact that the asymmetry of solar activity on long time scales (years, cycle phases, whole cycles) is an artifact caused by the utilization of inadequate indices.
- Even if the asymmetry is practically missing during the maximum phases of SCs, for the activity “pulses” on the descendant phases the values of the asymmetry increase towards one or the other hemispheres. This fact could be determined to the presence on the solar disk of some active regions with a lifetime greater than a solar rotation period.
- The strange behaviour of SXR flare activity on SC 22 descending phase could be the cause of the "abnormal" appearance of SC 23, i.e., the new magnetic dipole begins to lose part of its energy even during the descending phase of SC 22. Consequently, the activity of SC 23 proves to be well below the predicted values.
- Finally, we consider that the detailed study of the descending and the minimum phases of the SCs, at the stage when magnetic phenomena from both the old and the new cycle interact in the solar atmosphere, would be useful for inferring information about the activity level of the next cycle.

Acknowledgements. We acknowledge WDC-A for Solar-Terrestrial Physics, NOAA, Boulder, Colorado, for providing the data used in this study.

REFERENCES

- [1] ATAÇ, T., ÖZGÜÇ, A., Flare Index during the Rising Phase of Solar Cycle 23, *Solar Phys.*, **166**, 201, 1996.
- [2] ATAÇ, T., ÖZGÜÇ, A., North-South Asymmetry in the Solar Flare Index, *Solar Phys.*, **198**, 399, 2001.
- [3] BABCOCK, H. W., BABCOCK, H. D., The Sun's Magnetic Field, 1952-1954, *Astrophys. J.*, **121**,

349, 1955.

- [4] BAI, T., Distribution of Flares on the Sun – Superactive Regions and Active Zones of 1980-1985, *Astrophys. J.*, **314**, 795, 1987.
- [5] BAI, T., Distribution of Flares on the Sun during 1955-1985 – ‘Hot Spots’ (Active Zones) Lasting for 30 years, *Astrophys. J.*, **328**, 860, 1988.
- [6] DINULESCU, S., DINULESCU, V., Flare Activity during Solar Cycle 21, *Rom. Astron. J.*, **1**, 63, 1991.
- [7] GARCIA, H. A., Evidence for Solar-cycle Evolution of North-south Flare Asymmetry during Cycles 20 and 21, *Solar Phys.*, **127**, 185, 1990.
- [8] GNEVYSHEV, M. N., OHL, A. I., *Astron. Zh.*, **25**, 18, 1948.
- [9] KLECZEK, J., *Publ. Inst. Centr. Astron.*, **22**, 74, 1952.
- [10] KNOŠKA, Š., Distribution of Flare Activity on the Solar Disk in the Years 1937–1976, *Contr. Astrophys. Obs. Skalnaté Pleso*, **13**, 217, 1985.
- [11] KUKLIN, G. V., Cyclical and Secular Variations of Solar Activity, in V. BUMBA AND J. KLECZEK (eds.), Proc. UAI Symp. No. 71, “Basic Mechanisms of Solar Activity”, Prague, Czechoslovakia, 25–29 August 1975, D. Reidel Publ. Comp., Dordrecht, 147, 1976.
- [12] JONES, H. P., BRANDSTON, D. D., JONES, P. B., POPESCU, M. D., Comparison of Total Solar Irradiance with NASA/National Solar Observatory Spectromagnetograph Data in Solar Cycles 22 and 23, *Astrophys. J.*, **589**, 658, 2003.
- [13] LI, K. J., WANG, J. X., XIONG, S. Y., LIANG, H. F., YUN, H. S., GU, X. M., Regularity of the North-South Asymmetry of Solar Activity, *Astron. Astrophys.*, **383**, 648, 2002.
- [14] MARIȘ, G., in *Anuarul Astronomic*, Ed. Acad. Rom., Bucharest, (in Romanian) p. 319, 1987.
- [15] MARIȘ, G., POPESCU, M. D., ONCICA, A., DONEA A. C., Solar Activity Level on the Ascending Phase of the Solar Cycle 23, in: Proc. First Solar & Space Weather Euroconf., “The Solar Cycle and Terrestrial Climate”, Santa Cruz de Tenerife, Spain, 25–29 Sept. 2000 (**ESA SP-463**), p. 39, 2000.
- [16] MARIȘ, G., ONCICA, A., POPESCU, M. D., The 22-year Solar Magnetic Cycle. I. Sunspot and Radio Activity, *Rom. Astron. J.*, **11**, 13, 2001.
- [17] MARIȘ, G., POPESCU, M. D., ONCICA, A., DONEA, A.C., Solar Activity Level on the Ascending Phase of the Solar Cycle 23, in: Proc. “The Solar Cycle and Terrestrial Climate”, Santa Cruz de Tenerife, Spain, 25-29 September 2000, (**ESA SP-463**), 371, 2002a.
- [18] MARIȘ, G., POPESCU, M. D., MIERLA, M., Geomagnetic Consequences of the Solar Flares during the Last Hale Solar Cycle (II), in: Proc. “SOLSPA 2001: The Second Solar Cycle and Space Weather Euroconference”, Vico Equense, Italy, 24–29 September 2001, (**ESA SP-477**), 451, 2002b.
- [19] MARIȘ, G., POPESCU, M. D., DONEA, A.C., MIERLA, M., The 22-year Solar Magnetic Cycle. II. Flare Activity, in: G. MARIȘ AND M. MESSEROTTI (eds.), Proc. Regional Meeting “Solar Researches in the South-Eastern European Countries: Present and Perspectives”, Bucharest, Romania, 24–28 April 2001, *Observations Solaires 2002*, Ed. Acad. Rom., Bucharest, 48, 2002c.
- [20] MARIȘ, G., POPESCU, M. D., MIERLA, M., The North-South Asymmetry of Soft X-Ray Solar Flares, *Rom. Astron. J.*, **9**, 131, 2003.
- [21] POPESCU, M. D., MARIȘ, G., Space Weather, in: *Anuarul Astronomic 2002*, (in Romanian), Ed. Acad. Rom., Bucharest, 200, 2002.
- [22] POPESCU, M. D., MARIȘ, G., ONCICA, A., MIERLA, M., Flare Activity and the Strength of Solar Cycles, in: Proc. 10th European Solar Physics Meeting “Solar Variability: From Core to Outer Frontiers”, 9–14 September 2002, Prague, Czech Republic (**ESA SP-506**), 721, 2002.
- [23] TEMMER, M., VERONIG, A., HANSLMEIER, A., OTRUBA, W., MESSEROTTI, M., Statistical Analysis of Solar H_α Flares, *Astron. Astrophys.*, **375**, 1049, 2001.
- [24] TEMMER, M., VERONIG, A., HANSLMEIER, A., OTRUBA, W., MESSEROTTI, M, in: Proc. “SOLSPA 2001: The Second Solar Cycle and Space Weather Euroconference”, Vico Equense, Italy, 24–29 Sept. 2001, (**ESA SP-477**), 187, 2002.
- [25] VERMA, V. K., PANDE, M. C., UDIN, W., Energetic Flares on the Sun, *Solar Phys.*, **112**, 341, 1987.

- [26] VERMA, V. K., The Distribution of the North-South Asymmetry for the Various Activity Cycles, in: Proc. National Solar Observaroty/Sacramento Peak 12th Summer Workshop, *ASP Conf. Series*, **27**, 429, 1992.
- [27] VIZOSO, G., BALLESTER, J. L., The North-South Asymmetry of Sunspots, *Astron. Astrophys.*, **229**, 540, 1990.

Figure Captions

Caption Fig. 1 – The butterfly diagram for X-ray flares (1986 – 2001): C-type flares, upper panel; M & X-type, bottom panel); (on the data provided by WDC-A for Solar –Terrestrial Physics, NOAA E/GC2, Broadway, Boulder Colorado 80303, USA).

Caption Fig. 2 – The butterfly diagram for H_{α} flares (1994 – 2001); (on the data provided by WDC-A for Solar –Terrestrial Physics, NOAA E/GC2, Broadway, Boulder Colorado 80303, USA).

Caption Fig. 3 – The monthly distributions of the X-ray flares during January 1986 – March 2001 (C-type flares, upper panel; M & X-type, middle panel; C, M & X type, bottom panel).

Caption Fig. 4 – The monthly variations of the Q_x index for the X-ray flares (upper panel) and the Q index for H_{α} flares (bottom panel) during the period January 1986 – March 2001.

Caption Fig. 5 – The smoothed monthly mean values of: the Q index (magnified by 10), the Q_x index (magnified by 100); the sunspot numbers during the period July 1976 – Dec. 2001

Caption Fig. 6 – The annual values of the Q index and of the Q_x index (magnified by 10) and the annual sunspot numbers during the interval 1976–2001.

Caption Fig. 7 – The smoothed curves of the N-S asymmetry for Q_x and N indices.

Caption Fig. 8 – The annual N-S asymmetry of N and Q_x indices.

Figure 1

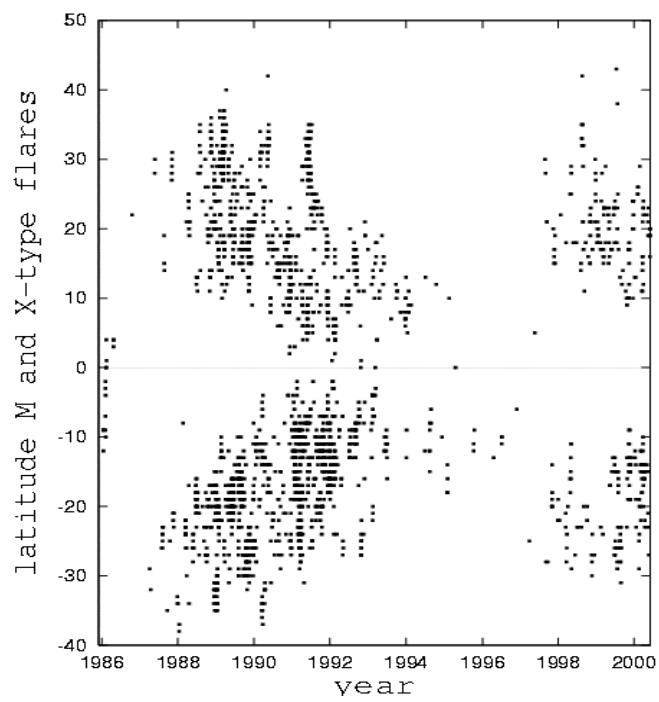
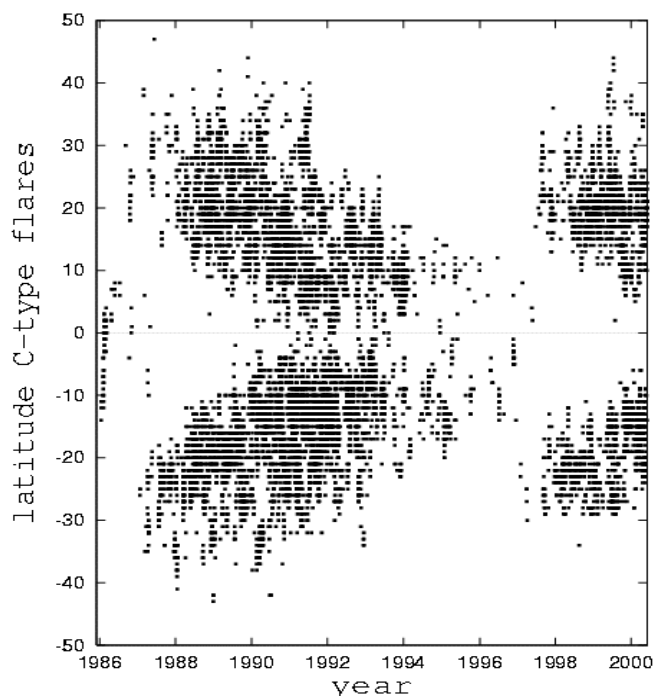


Figure 2.

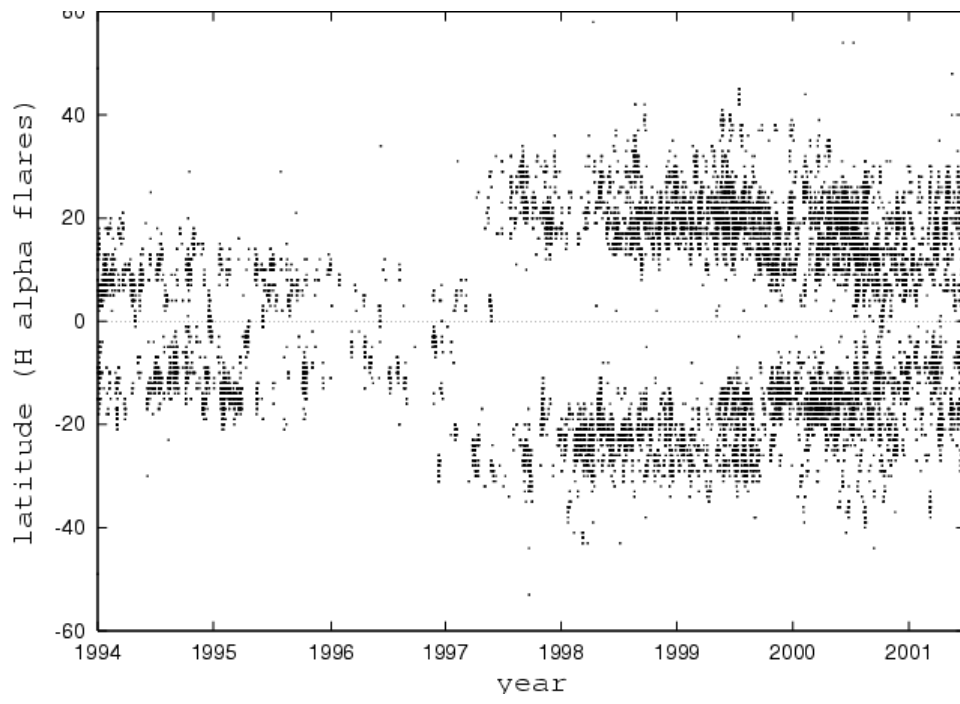


Figure 3.

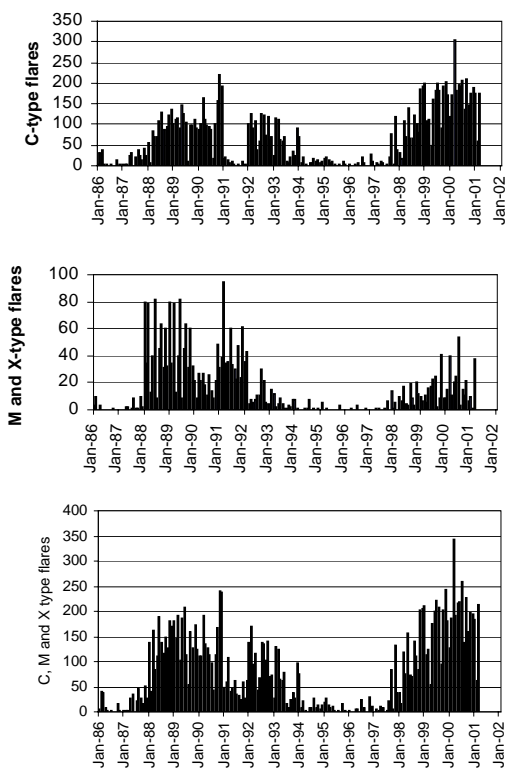


Figure 4.

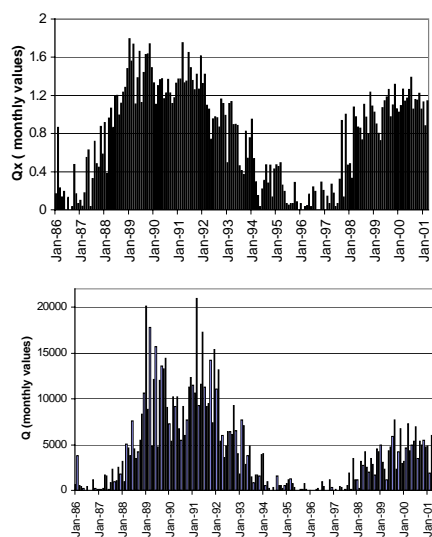


Figure 5.

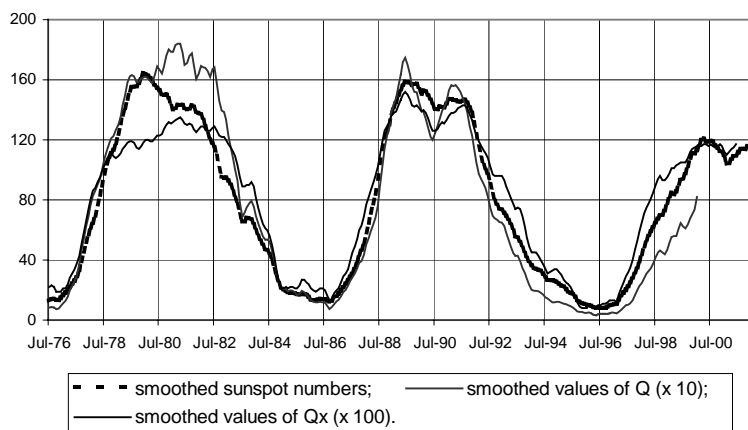


Figure 6

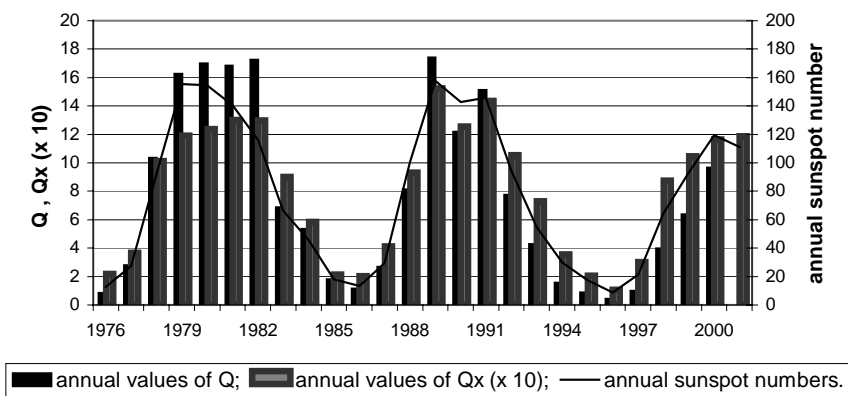


Figure 7.

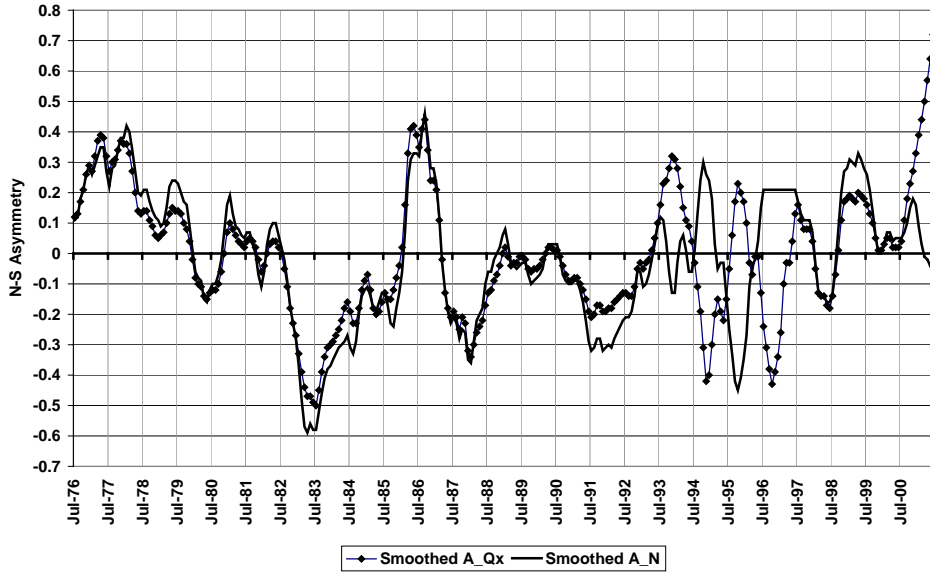


Figure 8.

